Original article
UDK 544.773

MECHANORESPONSIVE IONIC ELASTOMERS WITH ULTRA-STRETCHABILITY, HIGH TOUGHNESS, FATIGUE RESISTANCE, AND EXTREME TEMPERATURE RESISTANCE

Mai Xianmin[1], Kuzin Victor [2], Wang Ning [3]

[1] Southwest Minzu University, Chengdu, China
[2] Russian Academy of Engineering, Moscow, Russia
[3] Hainan University, Haikou, China
[*] E-mail: maixianmin@foxmail.com

Abstract. In the development of elastic materials, the non-synergy between stretchability and toughness is a challenge. Herein, we propose a rational design of a composite hydrogel by introducing strongly polarized hydrated Li-ion clusters, electron-withdrawing carboxyl groups, and Sn (II) complexation into hydrogen-bonded poly (acrylamide) (PAM) network. Weak interaction between Li-ions and amide groups facilitates the rapid flipping and slipping of the PAM chains during stretching, optimizing the stretchability of the hydrogel. This composite also provides an energy-dispersing mechanism based on strong ionic complexation between Sn (II) and amide groups, which improves its toughness. As-prepared composite hydrogel simultaneously exhibits high stretchability (> 7000% elongation), ultra toughness of 580 kPa, excellent fatigue resistance and extreme temperature resistance (elastic at −60 and 70 °C). Due to its excellent comprehensive performances, the present soft material has broad application prospects in agriculture, medicine, construction, and machinery.

Keywords: *polymer hydrogels; high stretchability; ionic complexation; anti-freezing; heat resistance.*

For citation: Mai X., Kuzin V., Wang N. Mechanoresponsive ionic elastomers with ultra-stretchability, high toughness, fatigue resistance, and extreme temperature resistance. *Journal of Science and Education of North-West Russia*. 2023. V.9. No. 2. pp. 64–75.

Научная статья
УДК 544.773

МЕХАНОРЕАКТИВНЫЕ ИОННЫЕ ЭЛАСТОМЕРЫ СО СВЕРХРАСТЯЖИМОСТЬЮ, ВЫСОКОЙ УДАРНОЙ ВЯЗКОСТЬЮ, СТОЙКОСТЬЮ К УСТАЛОСТИ И ЭКСТРЕМАЛЬНЫМ ТЕМПЕРАТУРАМ

Май Сяньминь [1], Кузин Виктор [2], Ван Нин[3]

[1] Юго-Западный национальный университет, Чэнду, Китай
[2] Российская инженерная академия, Москва, Россия
[3] Хайнаньский университет, Хайкоу, Китай
[*] E-mail: maixianmin@foxmail.com

Аннотация. При разработке эластичных материалов отсутствие синергии между способностью к растяжению и ударной вязкостью является проблемой. Здесь мы предлагаем рациональную конструкцию композитного гидрогеля путем введения сильно поляризованных гидратированных кластеров Li-ионов, электроноакцепторных карбоксильных групп и комплексо-образования Sn (II) в водородно-связанную поли (акриламидную) сетку (PAM).

Слабое взаимодействие между ионами Li и амидными группами способствует быстрому переворачиванию и проскальзыванию цепей PAM во время растяжения, оптимизируя растяжимость гидрогеля. Этот композит также обеспечивает механизм рассеивания энергии, основанный на сильном ионном комплексо-образовании между Sn(II) и амидными группами, что повышает его ударную вязкость. Полученный композитный гидрогель одновременно обладает высокой растяжимостью (относительное удлинение>7000%), сверх-прочностью 580 кПа, превосходной стойкостью к усталости и экстремальным температурам (эластичен при -60 и 70°C). Благодаря своим превосходным комплексным характеристикам, данный мягкий материал имеет широкие перспективы применения в сельском хозяйстве, медицине, строительстве и машиностроении.

Ключевые слова: *полимерные гидрогели; высокая растяжимость; ионное комплексо-образование; защита от замерзания; термостойкость*

Для цитирования: Май С., Кузин В., Ван Н. Механо-реактивные ионные эластомеры со сверх-растяжимостью, высокой ударной вязкостью, стойкостью к усталости и экстремальным температурам // Вестник науки и образования Северо-Запада России. 2023. Т.9. № 2. С. 64–75.

1. Introduction

Hydrogels, composed of inter-crosslinked polymer networks and water, play a key role in many applications of materials science, such as artificial skin, biological tissue engineering, biomedical devices, drug delivery, flexible electronic components, and self-healing architecture [1-3]. Polymer hydrogels are prepared through self-driven intermolecular non-covalent interactions, that is the hydrophobic effects, van der Waals forces, hydrogen bonds, π–π interactions, and electrostatic interactions [4,5]. Typical representatives include sliding-ring[6], double-network [7,8], topological [9], nanocomposite [10,11], ionic bond [12], macromolecular microsphere composite [13,14], and hydrophobic association hydrogels (HAH) [15,16]. Despite the remarkable progress in the development of multi-functional polymer hydrogels in recent decades, their practical applications have been limited due to the non-synergistic relationship between stretchability and toughness. For example, the PAM-based hydrogel exhibited a tensile strength as high as 1,500 kPa, owing to the copolymerization of acrylamide (AAM) and acryloyl pluronic 127 micelles, but its fracture strain was only 435% [17]. The Fe(III)/dimethylsiloxane (PDMS) material could be stretched more than 100 times without breaking, but its tensile stress was as low as 10 kPa [18].

Moreover, it is difficult for most polymer hydrogels to maintain mechanical longevity in high- or low-temperature environments, due to the inevitable evaporation or crystallization of liquid water. For example, the PAM-based HAH hydrogel transformed from an ultra-elastic material with a 3,500% fracture strain to a white rigid material with little water after being placed at 25 °C under a relative humidity of 65% for 24 h [19]. Designing high-quality polymer hydrogels with high stretchability and toughness in extreme temperature/humidity environments remains a major challenge for realizing their practical applications.

Herein, we report the design of an ultra-elastic composite hydrogel by introducing water-soluble lithium terephthalate (PTALi) and self-dispersing stannous terephthalate (PTASn) nanoparticles into hydrogen-bonded PAM networks. The weak interaction between the hydrated Li-ion clusters and amide groups allows the PAM chains to break and reform rapidly during stretching, resulting in the soft material with high stretchability (6640% fracture strain). Simultaneously, toughness of the polymer hydrogel is enhanced to 670 kPa, owing to the island-like PTASn nanoparticles, hydrogen bonds of carboxyl-amide groups and ionic complexation of Sn(II)–amide groups. This soft material changes the conventional perception that stretchability and toughness are not synergistic. Therefore, this composite hydrogel is suitable for a variety of applications such as stress sensors, biological muscles, medical drug carriers, repairable building materials, and vulcanized rubber substitutes.

2. Experimental

2.1. Material

All chemicals and solvents were of analytical grade and used without further purification. Acrylamide (99.0%), terephthalic acid (PTA, 99.0%), lithium hydroxide (Li OH, 99.5%), stannous chloride ($SnCl_2$, 20 g L^{-1}), hexadecyl trimethyl ammonium bromide (99.0%), hexadecyl methacrylate (95%), sodium chloride (NaCl, 99.5%), potassium sulfate (99.5%) and *N, N, N', N'*-tetramethylenediamine (99.5%) procured from by Aladdin (Shanghai, China).

2.2. Preparation of ALS hydrogels

Hydrophobically associating hydrogels were prepared by in-situ polymerization [21,22] CTAB (1 g) and NaCl (0.406 g) were dissolved in 20 ml deionized water by stirring until a clear solution was obtained. A saturated solution of 10 ml PTA Li was prepared using an equivalent ratio of Li OH and PTA, and then added to the above solution. A solution of stannous chloride (3 ml) was added to prepare a creamy PTAS gel, and stirred for 0.5 hour. HMA (0.254 ml) was then added to the micellar solution. After the solution was stirred at 25 °C for 5 h, 5 g AM, 0.02 g KPS and 0.052 ml TEMED were added to the highly dispersed micellar solution. Finally, the well-stirred mixture was poured into a customized glass mold and aged in a drying oven at 60 °C for 12 h to obtain hydrogel with 45 ± 5wt % of liquid water. Based on their composition, the as-prepared hydrogels are referred to as PAM, AL and ALS.

2.3. Performance characterization

Material characterization: FT-IR spectra were recorded on an FT-IR spectrometer (Nicolet 5700, USA) using freeze-dried hydrogel pellets (4,000–500 cm^{-1}). The surface morphology was investigated using FE-SEM (Hitachi S4800) and EDS (Bruker Nano X Flash Detector 5030). Before FE-SEM investigation, the samples were sputtered with gold. A Kratos AXIS-SUPRA spectrometer was used to analyze the XPS spectra (Zetasizer Nano S90) of the materials. Powder XRD measurements were performed at a scan rate of 4° min^{-1} and a step size of 0.03° in the 2θ range of 5° to 60°, using Cu Kα (λ=0.154056 nm) radiation. The ^1H CP/MAS NMR spectra were measured using a JEOL JNM-ECZ-600R spectrometer. TG analysis was performed at a heating rate of 10 °C min^{-1} from 35 to 800 °C in air, using a Q500 equipment. DSC heating and cooling curves were collected using a TADSC250 instrument, scanning from −90 °C to 0 °C at a scanning rate of 5 °C min^{-1} under nitrogen flow.

Mechanical Tests: Tearing testing was carried out using a commercial test tensile tester (MTS E44) with a 100 N load cell. The hydrogels were cut into standard dumbbell shapes of 2 mm thickness, 4 mm width and 5–20 mm gauge length. The two ends of the materials were clamped; one end was fixed, whereas the other end was pulled at 100–500 mm min^{-1}. The tearing energy is defined as the work required to tear a unit area, as estimated by $E = 2F/\lambda$, where F is the average force of peak values during steady-state tear, and λ is the width of the specimen.

Electrical signal characterization: Fresh ALS/LiCl hydrogels with an m_{PAM}/m_{LiCl} mass ratio of 5:3 were incubated in a cube of dimension 10 mm (length) × 4 mm (width) × 2 mm (thickness). The electrical resistance values of the sensors during mechanical deformation were measured using an electrochemical workstation (Shanghai Chenhua Instrument Co., Ltd., CHI660e). The sensing performance was evaluated by estimating the relative resistance change according to the equation $\Delta R/R_0 = (R–R_0)/R_0$, where R_0 corresponds to the resistance at the initial state, and R is assigned to the real-time resistance under a certain strain. The gauge factor is defined as $GF = (\Delta R/R_0)/\varepsilon$, where ε is the applied strain.

Molecular dynamics simulation: A periodic amorphous cell containing 20 PTA-Li chains, four PTA-Sn chains, five 20-repeating-unit PAM chains, and 200 water molecules was simulated using the Forcite module. The models were optimized using smart minimizer algorithm to obtain the lowest energy state. Molecular dynamics simulations of 10 ns NPT and 1000ps NVT ensembles were then performed on the initial cell. To calculate the cohesive energy density of each mixed

system, the models after the NVT ensemble simulation were optimized, and a 200ps molecular dynamics simulation was performed under the NVE ensemble.

3. Results and Discussion

3.1. Molecular Design, Mechanical Behavior and Structural Analyses of Mechanoresponsive Hydrogels

Chelation between Sn (II) and carboxyl group of terephthalate results in the formation of PTAS nanoparticles. Electrostatic repulsion of nanoparticles and coordination of Sn (II) with water molecules together form low-strength three-dimensional networks, thus exhibiting a long-term stable creamy gel in the macroscopic state (Figure S1, Supporting Information). We selected the PTA Li/PTA Sn gel to participate in the polymerization of AAM. The preparation was rather simple process of mixing AAM, PTA Li, $SnCl_2$, and water (mass ratio of 5:2:1:20) with potassium sulfate (KPS) chain initiator and *N*, *N*, *N′*, *N′*- tetramethylenediamine (TEMED) crosslinking agent, followed by thermal-induced polymerization of AAM at 60 °C for 12 h. The addition of PTA Li/PTA Sn gel serves three purposes, as shown Fig. 1: (f) weak interaction between the hydrated Li-ion clusters and amide groups improves the stretchability of the hydrogen-bonded PAM hydrogel. (ii) The hydrogen bond between carboxyl and amide groups drives the stiffening of the random-coil PAM chains. (iii) The strong ionic complexation between Sn (II) and amide groups enables the self-dispersing PTA Sn nanoparticles to fully dissipate energy during dynamic crosslinking with PAM chains, resulting in a significant increase in the fracture stress of the ultra-flexible material.

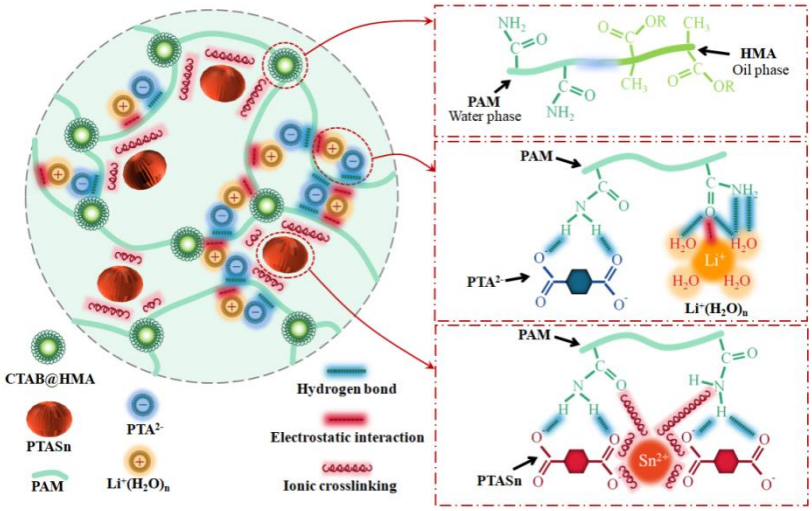

Fig. 1 Design strategy for ultra-stretchable and high-tough hydrogels

HAH hydrogels were selected as support materials due to their high stretchability of 1000–3500% [20,21]. Hexadecyl methacrylate (HMA) was uniformly dispersed in water with the help of hexadecyl trimethyl ammonium bromide (CTAB) surfactant to form CTAB@HMA micelle particles. The micelles are used as the points of association to connect the PAM polymer to form a flexible gel network structure [22,23]. In this work, PAM polymer hydrogels are transformed into ultra-flexible ALS soft materials (over 6000% fracture strain) under the weak interaction of electrostatic field. Simultaneously, the PAM chains are dynamically fixed on the surface of PTA Sn nanoparticles through strong ionic complexation, endowing the polymer hydrogel with a fracture stress of up to 670 kPa. Based on a reasonable combination of bond interactions, the as-prepared ALS polymer hydrogel exhibits fracture strength 26 times that of the soft materials with the same stretchable.

We evaluated the mechanical properties of the as-prepared PAM/PTA Li/PTA Sn (ALS) hydrogel. Fig. 2 shows representative stress–strain curves for fresh composite hydrogels of 2 mm thickness, 4 mm width, and 5–10 mm gauge length. Herein, we choose HAH hydrogel as the

flexible matrix material, based on the hydrophobic association effect (covalent bond property) between micellar particles and PAM chains. The polymer network of the HAH hydrogel is folded and bent, which allows a large chain extension during stretching. Therefore, the fracture strain of PAM HAH hydrogel is as high as 3200% in Fig. 2b. On this basis, the water-soluble PTA Li was used to further improve the tensile properties of PAM hydrogel. The ALS hydrogel with a water content of 45 ± 5wt % can be stretched up to 6640% (Fig. 2b and Figure S2), which is obviously higher than that of typical HAH hydrogels (1000–3500%) [20-23]. Among the PAM/MCl (M = Ca, Co, Mg, Na and Li) hydrogels with an m_{PAM}/m_{MCl} mass ratio of 1:1, the PAM/LiCl hydrogel exhibits the most excellent stretchability (5330%) in Fig. 2d. Fig. 2e further shows that Li-ion is the key to enhancing the stretchability of PAM hydrogels. There is a "bond" between the strongly polarized cations such as Li^+ and the carbonyl group of the PAM by virtue of electrostatic interaction. It is confirmed that the "lithium bond" weakens the intensity of the characteristic peak of carbonyl group in the fresh PAM/PTA Li (AL) and ALS hydrogels (Figure S3, Supporting Information). The weak coordination between Li-ion and amide group results in three-dimensional cross-linking of the PAM chains, which may lead to the break/re-formation of lithium bond during stretching. As a result, the AL and ALS hydrogels exhibit amazing super tensile properties (Table S1). To the best of our knowledge, the most stretchable polymer gels reported so far exhibit a high strain of 4000–10000% (Fig. 2f), corresponding to a fracture stress as low as 250–5 kPa [7,18-32]. The tensile stress of the fresh ALS hydrogel is as high as 670 kPa, which is more than 26 times that of the gel materials with the same stretch stability [18,32]. The ALS hydrogel provides multiple energy dissipation mechanisms, via the highly dispersed PTAS nanoparticles, hydrogen bonds of the carboxyl-amide groups, and ionic complexation between the Sn-ions and amide groups. Consequently, the as-prepared hydrogel exhibits ultra toughness, with a fracture energy of ~221 ± 20 kJ m^{-2} (Fig. 2c). Notably, well-designed ALS hydrogel can escape the theoretical constraints of non-synergy between stretchability and toughness.

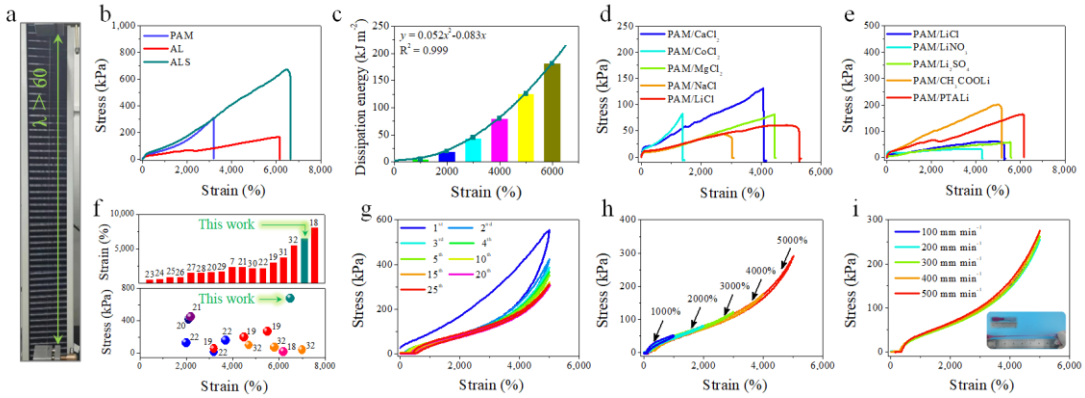

Fig. 2 Mechanical performances of the ALS hydrogels

(a) Representative tensile photograph of the soft material. (b) Initial stress–strain curves of the fresh PAM, AL and ALS hydrogels. (c) Corresponding strain–dependent dissipation energy of the ALS hydrogel during the first stretch. (d) Stress–strain curves of the PAM hydrogels with $CaCl_2$, $CoCl_2$, $MgCl_2$, NaCl and LiCl. (e) Stress–strain curves of the fresh hydrogels with different lithium salts. (f) A comparison of stress-strain between self-prepared ALS hydrogel and soft materials reported in the literature [7,18-32]. (g) Stress–loading/unloading curves of the ALS hydrogel at a fixed maximum strain of 5000% for 25 cycles without relaxation time. (h) Successive tensile loading–unloading curves of the ALS hydrogel as stretched to different strains. (f) Stress–strain cyclic curves at stretching rates of 100–500 mm min^{-1}. Note: the test sample has a standard dumbbell shape with a thickness of 2 mm, a width of 4 mm and gauge length of 5–10 mm.

The anti-fatigue behavior of the ALS hydrogel was studied by subjecting it to 25 consecutive loading-unloading cycles at a maximum strain of 5000%, as shown in Fig. 2g. After the initial cycle, the tensile curves become narrower and remain almost constant until a steady state is

reached in the following cycles, indicating the excellent elastic recovery of this material. As shown in Fig. 2h and Figure S4, cyclic stretching of the ultra-flexible hydrogel with increasing strain reproduces almost identical curves to the single tensile curve, and elastic recovery reaches approximately 98% as the strain is released from 1000% to 5000%. The stretchability of elastic materials is largely dependent on the stretching speed [33,34], but the as-prepared ALS hydrogel maintains nearly completely coincident stress–strain cyclic curves at stretching rates of 100–500 mm min^{-1} (Fig. 2i). The fatigue resistance tests further reveal the good toughness of the ALS hydrogel.

To understand the high toughness mechanism of the ALS hydrogel, we employed X-ray diffraction (XRD), Fourier-transform infrared spectroscopy (FT-IR), proton nuclear magnetic resonance (^{1}H NMR), X-ray photoelectron spectroscopy (XPS), thermogravimetric analysis (TG) and differential scanning calorimetry (DSC), and the results are summarized in Fig. 3 and Figure S5. Prior to the XRD measurement, the hydrogels were freeze-dried in a vacuum environment at −60 °C for 48 h, and corresponding XRD patterns are shown in Figure S6. The milky white PAM gel shows a series of diffraction peaks, which indicated that the PAM polymer crystallizes through intramolecular and/or intermolecular interaction forces (hydrogen bonds and van der Waals forces). However, any characteristic diffraction peaks cannot be observed in the ALS material, as the ionic complexation retains the three-dimensional network structure of the PAM chains. The FTIR spectrum of anhydrous PAM gel exhibits two distinct peaks at 1650 and 1470 cm^{-1}, corresponding to ν(C=O) and ν(C–N), respectively. Another peak is observed at 1575 cm^{-1}, which is attributed to $\nu(COO^-)$ of PTA Li. For the dried ALS sample, both ν(–C=O) and ν(C–N) of PAM shift to higher wavenumbers, whereas $\nu(COO^-)$ of the terephthalate salts is almost unchanged (Figure S7, Supporting Information). This ionic complexation is further evidenced by comparing the ^{1}H NMR spectra of PAM, AL, and ALS dissolved in D_2O (Fig. 3b), which shows that the complexation-related H_1 resonance peaks from PAM exhibits a remarkable chemical shift.

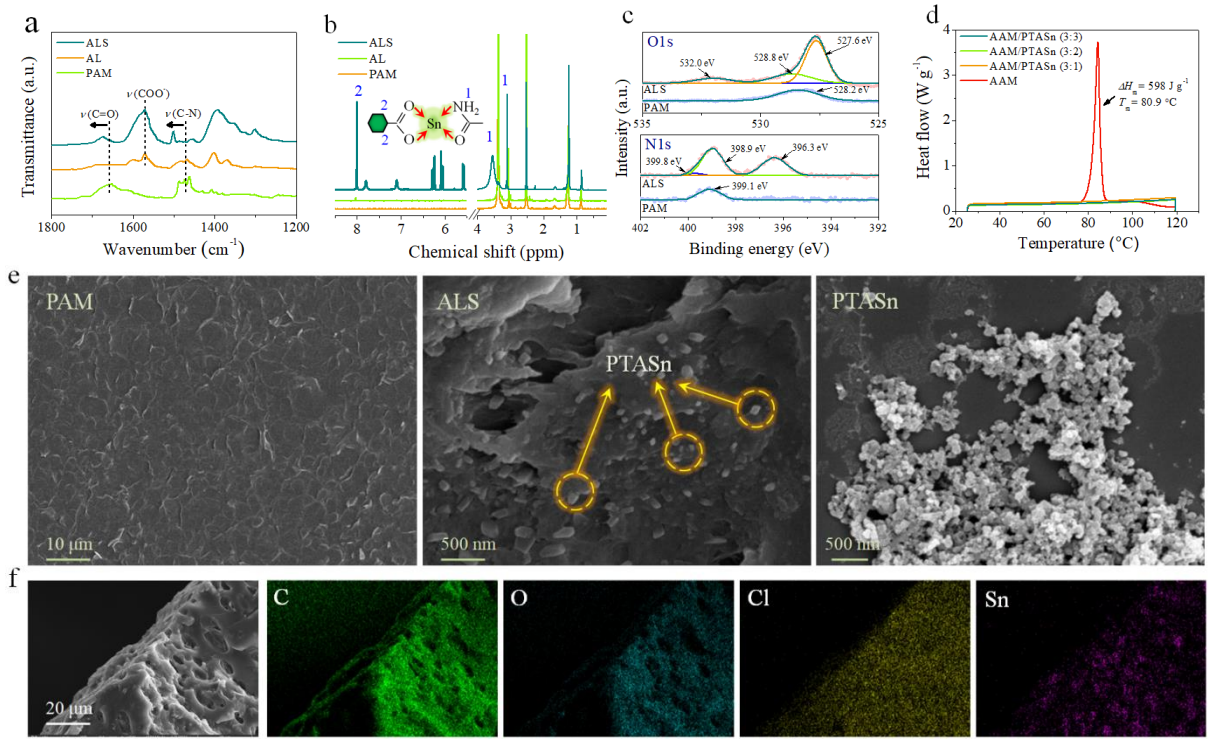

Fig. 3 Internal interactions of the ALS hydrogels

(a) FTIR spectra of the anhydrous PAM, AL and ALS samples. (b) ^{1}H CP-MAS NMR spectra. (c) High-resolution XPS spectra of N1s and O1s of the PAM and ALS hydrogels. (d) DSC curve of AAM and AAM/PTA Sn samples. (e) FE-SEM images of the PAM, ALS and extract of PTA Sn. (f) Elemental mapping by EDX for the ALS hydrogel revealing a uniform distribution of Sn element.

Furthermore, both the O1s and N1s spectra of PAM are clearly split and shifted in the case of the ALS gel (Fig. 3c and Figure S8). DSC curves of the AAM/PTA Sn mixture (Fig. 3d) were tested to further verify the ionic complexation between Sn (II) and amide groups. AAM exhibits a sharp endothermic peak between 78−90 °C, corresponding to a sublimation heat of 598 J g^{-1}. However, it is impossible to observe any sharp peaks in the AAM/PTA Sn mixtures within the same temperature range because the ionic complexation between Sn (II) and amide group limits the sublimation of AAM. Field emission scanning electron microscopy (FE-SEM) and energy-dispersive spectroscopy mapping (EDS-mapping) of the anhydrous gels were performed to analyze the microscopic morphology of the ALS material (Fig. 3e and Figure S9−S11). It is apparent that a large number of PTA Sn particles (about 50 nm) are dispersed in the continuous phase of PAM, forming typical sea-island structures, which plays the role of internal plasticization and acts as the ionic complexation.

To further profile the toughness strengthening process, we performed a molecular dynamics simulation of this process by stretching a periodic amorphous cell containing 20 PTA Li chains, four PTA Sn chains, five 20-repeating-unit PAM chains, and 200 water molecules. As shown in Figure S12, PAM appears as a random-coil chain surrounded by the PTA Sn and water molecules, corresponding to an energetically stable soft network of ALS hydrogel (total energy = −14701.0 kJ mol^{-1}; electrostatic energy = −19646.2 kJ mol^{-1}). For the PAM hydrogel network, total energy and electrostatic energy are equal to -4119.3 and -6273.6 kJ mol^{-1} (Figure S13, Supporting Information), respectively, implying that this material is far less stable than the ALS network. When the hydrogel is stretched to 200%, the PAM chain is strongly extended along the stretching direction, and the PAM-PTA Sn network reaches mechanical equilibrium again after sufficient relaxation, such that the energy of the ALS gel system remained almost unchanged (Figure S14, Supporting Information). As shown in Figure S15, the calculated values of the cohesive energy density also indicate that PTA Sn enhances the stability of the hydrogen-bonded PAM network via ionic complexation.

3.2. Anti-freezing and Heat Resistance Performances of the ALS/LiCl Hydrogels

We further employed a well-known hygroscopic material (LiCl) to enhance the moisturizing, anti-freezing, and heat-resistant properties of the ALS hydrogel. The PAM/PTA Li/PTA Sn/LiCl (ALS/LiCl) hydrogel composite with an m_{PAM}/m_{LiCl} mass ratio of 5:3 is stretched to over 70 times its original length without breaking (Fig. 4a-c). With the help of liquid water to promote the regeneration of all physical bonds, the artificial incision on the ALS/LiCl hydrogel film completely disappears at 25 °C after 6 h at a relative humidity of 90% (Fig. 4d). The ALS/LiCl hydrogels were dried at 60 °C to further examine the relationship between mechanical properties and water content (Fig. 4e). The fracture stress increases significantly with a decrease in water content and vice versa, but the fracture strain decreases rapidly. The water content remains at approximately 26% even after the composite is dried for 24 h, and the corresponding fracture strain and stress are 1420% and 1360 kPa, respectively. Moreover, the water content of the fresh ALS/LiCl hydrogel composite remains almost unchanged for a long time (28 d), due to the excellent moisturizing ability of lithium chloride. The ALS/LiCl hydrogels were placed in a high temperature environment of 50–70°C for 36 h to examine their heat resistance. The corresponding stress–strain curves are shown in Fig. 4f. Fracture strain of the hydrogel composite reaches 2840% after being heated at 50 °C, corresponding to a maximum stress of 1380 kPa. Oddly, the polymer hydrogel shows ultra-flexibility (360% of fracture strain, 7300 kPa of fracture stress) even after being dehydrated at 70 °C for 36 h, as shown in Fig. 4f and g. The ionic radius of Li-ions is only 0.6 nm, which is much lower than that of other alkali metal ions. Therefore, Li-ions exhibit hydration energies [35] as high as 120–150 kJ mol^{-1} (Figure S16 and Table S2). The water-locking effect of lithium chloride enables the polymer gel to exhibit excellent high-temperature resistance.

The phase diagram of the LiCl-water solution indicates that a solution with concentration in the range 25–30wt % cannot freeze when the temperature is –60 °C (Figure S17). This is demonstrated in the embedded graph (Figure 4i). The fresh ALS/LiCl hydrogel with an m_{PAM}/m_{LiCl} mass ratio of 5:3 retains its ultra-flexible properties at –60 °C. Its stretch ratio maintains at 420% at 25 °C, –30 °C and –60 °C under an external force of 0.5 N (Figure 4h). As indicated by Figure 4i, the initial stress–strain curves at different temperatures show striking similarities with each other, for a typical ALS/LiCl hydrogel with an m_{PAM}/m_{LiCl} mass ratio of 5:3. According to differential

scanning calorimetry (DSC) curves (Figure S18–S21, Supporting Information), the ALS/LiCl hydrogel does have any endothermic/exothermic peaks in the temperature range of –80 °C to 20 °C, indicating that the freezing point of the composite hydrogel is lower than –80 °C.

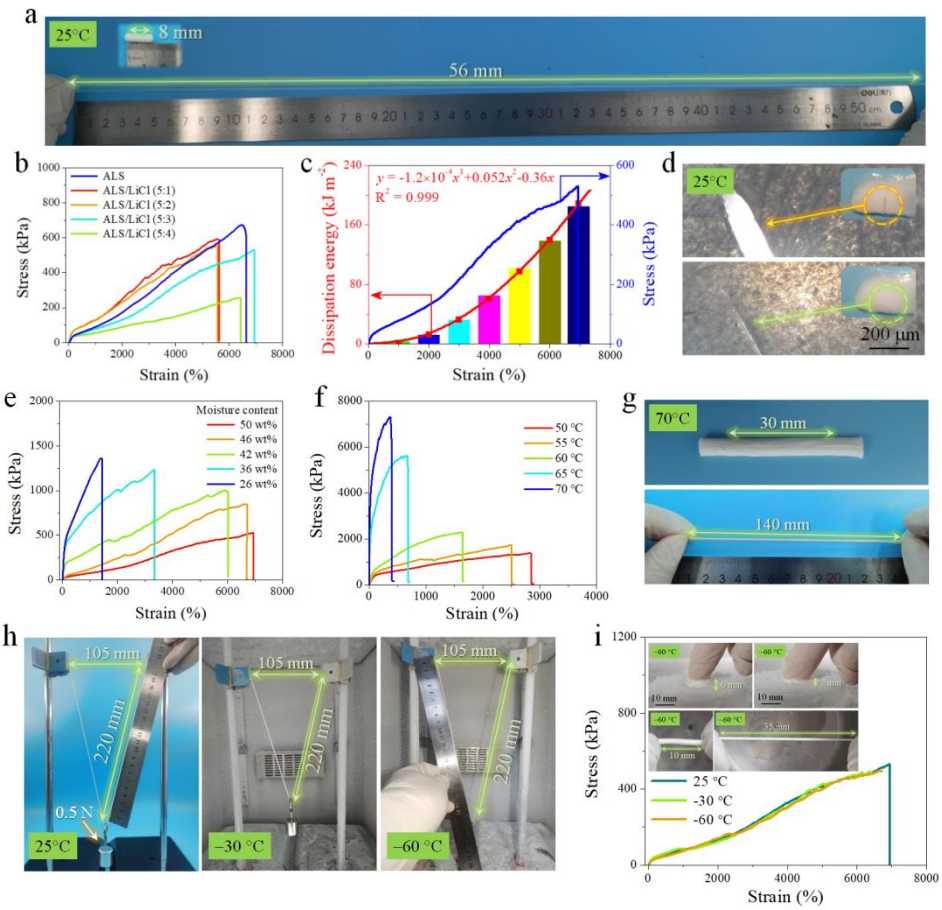

Fig. 4 Stress–strain, self-healing, moisture–preserving, anti-freezing, and heat resistant properties of the ALS/LiCl composite hydrogels

(a) Exhibition of superior stretchability for the ALS/LiCl hydrogel with an m_{PAM}/m_{LiCl} mass ratio of 5:3. (b) Stress–strain curves of the ALS/LiCl hydrogels with different mass ratios of m_{PAM}/m_{LiCl} (5:0, 5:1, 5:2, 5:3 and 5:4). (c) Corresponding strain–dependent dissipation energy of the ALS/LiCl composite hydrogel with an m_{PAM}/m_{LiCl} mass ratio of 5:3 during the first stretch. (d) Self-healing process of the ALS/LiCl hydrogel with an m_{PAM}/m_{LiCl} mass ratio of 5:3 at 25 °C after 6 h at a relative humidity of 90%. (e) Stress–strain curves of the ALS/LiCl soft material with an m_{PAM}/m_{LiCl} mass ratio of 5:3 after being placed at 60 °C for x (x = 1–24) h. (f) Tensile curves of the ALS/LiCl hydrogel with an m_{PAM}/m_{LiCl} mass ratio of 5:3 after being placed at 50–70 °C for 36 h. (g) Representative photograph of tensile testing of the soft material before/after being placed at 70 °C for 36 h. (h) Anti-freezing performances of the representative hydrogel with a diameter of 5 mm and an effective length of 105 mm under an external force of 0.5 N. (i) Tensile curves of the ALS/LiCl hydrogel with an m_{PAM}/m_{LiCl} mass ratio of 5:3 after being placed at –60 °C for 48 h. Note: Embedded photographs for the flexibility characterization of representative hydrogels at –60 °C for 48 h.

3.3. Conductivity of the As-Prepared ALS/LiCl Hydrogels

The as-prepared ALS/LiCl hydrogel with an m_{PAM}/m_{LiCl} mass ratio of 5:3 can serve as a sensor for detecting and monitoring a variety of external stimuli via electrical signals. For instance, its resistance changes increase nonlinearly with strain, as shown in Fig. 5a. The gauge factor (GF) increases unevenly from 0.6 to 5.2 as the strain increases to 2000%. Interestingly, the maximum resistance change rate of the hydrogel composite reaches 24000%, which is far superior to soft materials reported in the literature [7,36]. In Figure 5b, the stress–strain and voltage–strain curves are independent of the stretching speed, in the range 100–500 mm min^{-1}. The change in resistance

of the ultra-flexible hydrogel exhibits excellent stability and repeatability (Fig. 5d) during continuous stretching for 300 cycles at a large fixed strain of 3000% (Fig. 5c), thereby indicating its outstanding anti-fatigue properties. In addition, cyclic stretching of the ALS/LiCl hydrogel material at fixed strains of 1000, 2000, 2500, 3000, 3500 and 4000% produces repeatable and strain-dependent resistance changes, as shown in Fig. 5e. Ultra-flexible hydrogels have potential applications as strain sensors, owing to their striking tensile strain, excellent fatigue resistance, and reliable electrical signal response. The tensile strain is fixed at approximately 5500% and the electrical signal–tensile strain curve of the polymer hydrogel is shown in Fig. 5f.

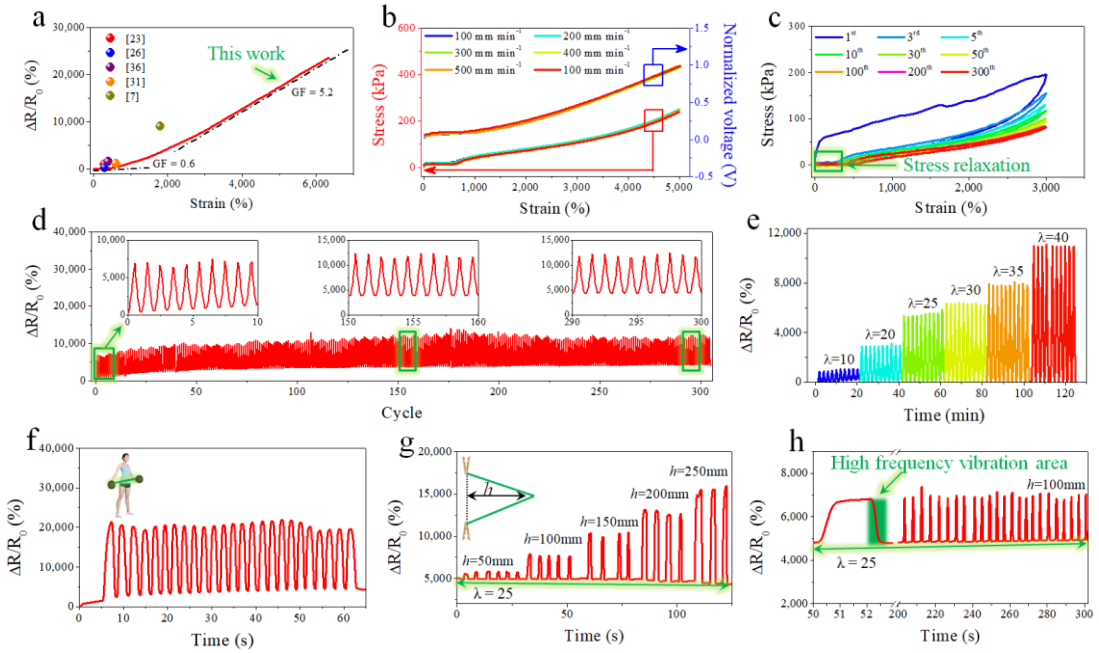

Fig. 5 Characterization of current–voltage signals of the ALS/LiCl hydrogel with an m_{PAM}/m_{LiCl} mass ratio of 5:3 during stretching

(a) Strain–dependent resistance changes of the composite hydrogel. (b) Stress–strain and voltage–strain curves at different stretching rates. (c) Stress–strain curves of the representative hydrogel after being stretched to 3000% strain for 300 cycles. (d) Relative resistance variations of the hydrogel with an m_{PAM}/m_{LiCl} mass ratio of 5:3 upon stretching to 3000% strain for 300 cycles. (e) Real-time response curves measured at fixed strains of 1000, 2000, 3000, 3500 and 4000% for ten cycles each. (f) Fast response to electrical signals during stretching. (g) Electrical signal characterization of the polymer hydrogels during shear motion when the stretched length was fixed at 2500%. (h) Electrical signal response of the composite hydrogel with an m_{PAM}/m_{LiCl} mass ratio of 5:3 when tangential displacement was fixed at 100 mm. Note: When the shear force was quickly withdrawn, the hydrogel exhibited a high-frequency vibration state. The real-time electrical signal response did not observe periodic fluctuations in the high-frequency vibration area.

Despite the rapid completion of 25 cycles within 55 s, the output electrical signal exhibits a stable periodic variation. The shear test can be described as a 10 mm gauge length of ionic elastomer that is first fixed and stretched to 250 mm, and then tangentially stretched 50–250 mm. As shown in Fig. 5g, the $\Delta R/R_0$ value of the ALS/LiCl hydrogel composite reproducibly increased from 5000% (2500% stretch) to 15500% at a shear displacement of 250 mm. The change in resistance of the ionic elastomer exhibits excellent stability and repeatability during continuous shear stretching for 25 cycles at a large fixed shear displacement of 100 mm (Fig. 5h), indicating its excellent durability. The afore mentioned results suggest the great potential of the as-prepared ALS/LiCl hydrogel composite for timely online detection of conductivity and pressure changes under ultra-high strain, which is important in fitness equipment, wearable electronic devices, anti-theft systems and monitoring building deformation.

Table 1. Comparison of the overall performance between this work and previously reported typical ultra-flexible materials.

Soft materials	Stretchability [%]	Toughness [kPa]	Anti-freezing [°C]	Heat Resistance [°C]	$\Delta R/R_0$ [%]	Refs.
PAA/betaine	1600	4500	–40	NA	9000	[7]
PAA/PDA/glycerol	600	60	–20	60	NA	[24]
PAN/PAM	850	2100	NA	NA	300	[26]
Fe-Hpdca-PDMS	6200	12	–20	NA	No	[18]
	10000	10	–20	NA	No	
PAM/$CaCl_2$	7000	25	–40	50	NA	[32]
	12500	7	–40	50	NA	
PT/PVA/Cl	500	510	NA	NA	950	[23]
PAM/PDA/PMEA	1050	42	NA	NA	1500	[36]
ALS/LiCl	>7000	>500	<–60	>70	24000	Our work

4. Conclusion

In this work, we successfully prepared a mechanoresponsive ALS/LiCl ionic hydrogel by introducing hydrogen-bonded PAM chains and self-dispersed PTA Sn nanoparticles to mimic the roles of soft organic networks and stiff calcium salts in natural fishbone, respectively. The dynamic nature of the electrostatic interaction, hydrogen bond, and ionic complexation with different interaction strengths, overcomes the inherent conflict between the stretchability and toughness of the PAM network. Compared to previously reported elastic polymer materials in Table 1, the as-prepared ALS/LiCl hydrogel shows extraordinary mechanical performance in terms of ultra-high stretchability (>7000%), excellent toughness (>500 kPa), good elastic recovery, frost resistance (<–60 °C), anti-heating performance (>70 °C), and hight sensitive electrical signal (24000% of $\Delta R/R_0$). This study discredits the traditional understanding of the non-synergistic nature of stress and strain in soft materials and provides a method for designing ultra-elastic hydrogels.

Acknowledgements

This work was supported by the Finance Science and Technology Project of Hainan Province (No. ZDYF2021SHFZ102 and ZDYF2020205), National Youth Talent Support Program, Hainan Science and Technology Major Project (No. ZDKJ2019013), National Natural Science Foundation of China (No. 51775152, 61761016, 22065012 and U1967213), National Key R&D Program of China (No. 2018YFE0103500), Start-up Research Foundation of Hainan University (No. KYQD(ZR)1911), and Project Supported by Open Project of State Key Laboratory of Marine Resource Utilization in South China Sea (Hainan University) (No. MRUKF2021025), Sichuan Provincial Youth Scientific and Technological Innovation Research Team on Ecological Adaptability of Plateau Architecture (No. 2022JDTD0008).

REFERENCES

1. Wang L., Daoud W.A. Hybrid conductive hydrogels for washable human motion energy harvester and self-powered temperature-stress dual sensor. Nano Energy. 2019, V. 66, 104080.

2. Luo X., Zhu L., Wang Y. C., Li J., Nie J., Wang Z.L. A flexible multifunctional triboelectric nanogenerator based on M Xene /PVA hydrogel, Adv. Funct. Mater. 2021, No 4, 2104928.

3. Nele V., Wojciechowski, J. P., Armstrong P. K., Stevens M. M., Tailoring gelation mechanisms for advanced hydrogel applications, Adv. Funct. Mater. 2020, V. 30, 2002759.

4. Li H., Sun H, Qian G., Li N., Yao Y., Chen T. Ultrastretchable and superior healable supercapacitors based on a double cross-linked hydrogel electrolyte. Nat. Commun. 2019, V. 10, 536.
5. Wang X., Pi M., Ran R. High-strength, highly conductive and woven organic hydrogel fibers for flexible electronics. Chem. Eng. J. 2022, V. 428, 131172.
6. Dikshit K., Bruns C. J. Post-synthesis modification of slide-ring gels for thermal and mechanical reconfiguration. Soft Matter. 2021, V. 17, 5248.
7. Zhang W., Wu B., Sun S., Wu P. Skin-like mechanoresponsive self-healing ionic elastomer from supramolecular zwitterionic network. Nat. Commun. 2021, V. 12, 4082.
8. Chen J., Huang J, Hu Y. 3D printing of biocompatible shape-memory double network hydrogels, ACS Appl. Mater. Interfaces. 2021, V. 13, 12726.
9. Liu D., G. Yin G., Le X., Chen T. Supramolecular topological hydrogels: from material design to applications, Polym. Chem. 2022, V. 13, 1940.
10. Jaiswal M. K., Xavier J. R., Carrow J. K., Desai P., Alge D., Gaharwar A.K. Mechanically stiff nanocomposite hydrogels at ultralow nanoparticle content. ACS, 2016, No 10, 246.
11. Zhao Z., Fang R., Rong Q., Liu M. Bioinspired nanocomposite hydrogels with highly ordered structures. Adv. Mater. 2017, V. 29, 1703045.
12. Liang Y., Xue J., Du B., Nie J. Ultrastiff, tough, and healable ionic-hydrogen bond cross-linked hydrogels and their uses as building blocks to construct complex hydrogel structures, ACS Appl. Mater. Interfaces. 2019, No 11, 5441.
13. Jiang F., Huang T., He C., Brow H. R., Wang H. Interactions affecting the mechanica properties of macromolecular microsphere composite hydrogels. J. Phys. Chem. 2013, V. 117, 13679.
14. Wang C., L. Yang L., He Y., Xiao H., Lin W. Microsphere-structured hydrogel crosslinked by polymerizable protein-based nanospheres. Polymer 211. 2020, No 4, 123114.
15. Na R., Liu Y., Lu N., Zhang S., Liu F., Wang G. Mechanically robust hydrophobic association hydrogel electrolyte with efficient ionic transport for flexible supercapacitors. Chem. Eng. J. 2019, V. 374, 738.
16. Gao Y., Gu S., Duan L., Wang Y., Gao G. Robust and anti-fatigue hydrophobic association hydrogels assisted by titanium dioxide for photocatalytic activity. Soft Matter. 2019, V. 15, 3897.
17. Li Y., Wang D., Wen J., Liu J., Zhang D., Li J., Chu H. Ultra-stretchable, variable modulus, shape memory multi-purpose low hysteresis hydrogel derived from solvent-induced dynamic micelle sea-island structure. Adv. Funct. Mater. 2021, V. 31, 2011259.
18. Li C.H., Wang C., Keplinger C., Zuo J. L., Jin L., Sun Y., Zheng P., Cao Y., Lissel F., Linder C. X. –Z. You, Z. Bao, A highly stretchable autonomous self-healing elastomer. Nat. Chem. 2016, No 8, 618.
19. Qiang C., Lin Z., Hong C., Yan H., Huang L., Yang J., Zheng J. A novel design strategy for fully physically linked double network hydrogels with tough, fatigue resistant, and self-healing properties, Adv. Funct. Mater. 2015, V. 25, 1598.
20. Chen Q., Yan X., Zhu L., Chen H., Jiang B., Wei D., Huang L., Yang J., Liu B., Zheng J. Improvement of mechanical strength and fatigue resistance of double network hydrogels by ionic coordination interactions. Chem Mater. 2016, V. 28, 5710.
21. Jiang B., Long Y., Pu X., Hu W., Wang Z. L. A stretchable, harsh condition-resistant and ambient-stable hydrogel and its applications in triboelectric nanogenerator. Nano Energy. 2021 V. 86, 106086.
22. Han L., Lu X., Wang M., Gan D., Deng W., Wang K., Fang L., Liu K., Chan C. W., Tang Y., Weng L.-T., Yuan H. A mussel-inspired conductive, self-adhesive, and self-healable tough hydrogel as cell stimulators and implantable bioelectronics, Small. 2017, V. 13, 1601916.
23. Zhang H., Tang N., Yu X., Guo Z., Liu Z., Sun X., Li M.-H., Hu J. Natural glycyrrhizic acid-tailored hydrogel with in-situ gradient reduction of Ag NPs layer as high-performance, multi-functional, sustainable flexible sensors. Chem. Eng. J. 2021, V. 430, 132779.

24. Han L., Liu K., Wang M., Wang K., Fang L., Chen H., Zhou J., Lu X. Mussel-inspired adhesive and conductive hydrogel with long-lasting moisture and extreme temperature tolerance. Adv. Funct. Mater. 2018 V. 28, 1704195.
25. Panda P., Dutta A., Ganguly D., Chattopadhyay S., R. K. Das R. K. Engineering hydrophobically associated hydrogels with rapid self-recovery and tunable mechanical properties using metal-ligand interactions. J. Appl. Polym. Sci. 2020, V. 137, 49590.
26. Shuai L., Guo Z. H., Zhang P., Wan J., Pu X., Wang Z. L., Stretchable, self-healing, conductive hydrogel fibers for strain sensing and triboelectric energy-harvesting smart textiles. Nano Energy. 2020 V. 78, 105389.
27. Huang Y., Zhong M., Shi F., Liu X., Tang Z., Wang Y., Huang Y., Hou H., Xie X., Zhi C. An intrinsically stretchable and compressible supercapacitor containing a polyacrylamide hydrogel electrolyte. Angew. Chem. Int. Ed. 2017, V. 56, 9141.
28. Pu X., Liu M., Chen X., Sun J., Du C., Zhang Y., Zhai J., Hu W., Wang Z. L. Ultrastretchable, transparent triboelectric nanogenerator as electronic skin for biomechanical energy harvesting and tactile sensing. Sci. Adv. 2017, No 3, 1700015.
29. Sun J.-Y., Zhao X., W. R. Illeperum W. R., Chaudhuri O., Oh K. H., Mooney D. J., Vlassak J. J., Suo Z. Highly stretchable and tough hydrogels. Nature. 2012, V. 489, 133.
30. Yuan N., Xu L., Wang H., Fu Y., Zhang Z., Liu L., Wang C., Zhao J., Rong J. Dual physically cross-linked double network hydrogels with high mechanical strength, fatigue resistance, notch-insensitivity, and self-healing properties. Acs Appl. Mater. Interfaces. 2016, No 8, 34034.
31. Liu L., Li X., Ren X., Wu G. F. Flexible strain sensors with rapid self-healing by multiple hydrogen bonds. Polymer. 2020, V. 202, 122657.
32. Zhang H., Liu Z., Mai J., Wang N., Liu H., Zhong J., Mai X. A smart design strategy for super-elastic hydrogel with long-term moisture, extreme temperature resistance, and non-flammability. Adv. Sci. 2021, No 8, 2100320.
33. Zhu F., Lin J., Wu Z. L., Qu S., Yin J., Qian J., Zheng Q. Tough and conductive hybrid hydrogels enabling facile patterning. Acs Appl. Mater. Interfaces. 2018, No 10, 13685.
34. Zheng S. Y., Ding H., Qian J., Yin J., Wu Z. L., Song Y., Zheng Q. Metal-coordination complexes mediated physical hydrogels with high toughness, stick–slip tearing behavior, and good processability. Macromolecules. 2016, V. 49, 9637.
35. Migliore M., Corongiu G., Clementi E., Lie G. C. Monte Carlo study of free energy of hydration for Li^+, Na^+, K^+, F^-, and Cl^- with ab initio potentials. J. Chem. Phys. 1988, V. 88, 7766.
36. Li S., Zhou H., Li Y., Jin X., Liu H., Lai J., Wu Y., Chen W. A Ma, Mussel-inspired self-adhesive hydrogels by conducting free radical polymerization in both aqueous phase and micelle phase and their applications in flexible sensors. J. Colloid Inter. Sci. 2022, V. 607, 431.

ИНФОРМАЦИЯ ОБ АВТОРАХ

Май Сяньминь – доктор техн. наук, профессор, Юго-Западный национальный университет ((610041, Китай, Ченду, e-mail: maixianmin@foxmail.com).
Кузин Виктор – доктор техн. наук, профессор, Российская инженерная академия (125993, Россия, Москва, e-mail: vfruzin@mail.ru).
Ван Нин – доктор техн. наук, профессор, Хайнаньский университет (650114, Китай, Хайкоу, e-mail: wangn02@foxmail.com).

INFORMATION ABOUT THE AUTHORS

Mai Xianmin – Dr. Sci. (Eng), Prof., Southwest Minzu University (610041, China, Chendy, e-mail: maixianmin@foxmail.com).
Kuzin Victor – Dr. Sci. (Eng), Prof., Russian Academy of Engineering, (125993, Russia, Moscow, e-mail: vfruzin@mail.ru).
Wang Ning – Dr. Sci. (Eng), Prof., Hainan University (650114, China, Haikou, e-mail: wangn02@foxmail.com).

Статья поступила в редакцию 15.03.2023; одобрена после рецензирования 10.04.2023, принята к публикации 07.05.2023.
The article was submitted 15.03.2023; approved after reviewing 10.04.2023; accepted for publication 07.05.2023.